

Unveiling the superconducting mechanism and phase stability of LaB_2H_8 under pressure

Jirun Wu(吴际润), Zefang Wang(王泽方), Xin Zhong(钟鑫), and Hanyu Liu(刘寒雨)
Citation: Chin. Phys. B, 2026, 35 (**5**): 057401. DOI: 10.1088/1674-1056/ae39d0
http://cpb.iphy.ac.cn; http://iopscience.iop.org/cpb

What follows is a list of articles you may be interested in

Manipulating the electronic structure and superconductivity of Li_2B_3C by biaxial strain

Yuhao Gu(顾雨豪), Yihao Wang(王奕淏), and Shuxian Hu(胡淑贤)
Chin. Phys. B, 2026, 35 (**4**): 047401. DOI: 10.1088/1674-1056/ae5594

High-throughput discovery and electron-doping tuning of superconducting ternary lithium borides

Bohan Cao(曹博瀚), Xinwei Wang(王新伟), Yibo Sun(孙一博), Mengxin Yang(杨孟鑫), Defang Duan(段德芳), Fubo Tian(田夫波), and Tian Cui(崔田)
Chin. Phys. B, 2026, 35 (**3**): 037401. DOI: 10.1088/1674-1056/ae27b1

Doping-dependent optical properties in YBCO superconducting films via $BaHfO_3$ nanocrystal addition

Shulun Han(韩淑伦), Yuanjie Ning(宁苑杰), Jing Chen(陈静), Yanqun Guo(郭艳群), Zicong Yang(杨子聪), Ping Zhu(朱萍), Zhigang Zeng(曾志刚), Chuanbing Cai(蔡传兵), Xinmao Yin(尹鑫茂), and Lijun Tian(田立君)
Chin. Phys. B, 2026, 35 (**2**): 027404. DOI: 10.1088/1674-1056/adee87

Exotic superconductivity in new topological kagome metal $CsTi_3Bi_5$

Jiali Liu(刘家利), Zhen Zhao(赵振), Hongqin Xiao(肖洪钦), Yuhang Zhang(张宇航), Zouyouwei Lu(鲁邹有为), Jihu Lu(卢佶虎), Feng Wu(吴凤), Chengjie Xu(徐诚杰), Hua Zhang(张华), Hui Chen(陈辉), Haitao Yang(杨海涛), Ziyi Liu(刘子儀), Xiaoli Dong(董晓莉), and Hongjun Gao(高鸿钧)
Chin. Phys. B, 2026, 35 (**2**): 027403. DOI: 10.1088/1674-1056/ae2c6d

Pressure-stabilized Li_2K electride with superconducting behavior

Xiao-Zhen Yan(颜小珍), Quan-Xian Wu(邬泉县), Lei-Lei Zhang(张雷雷), and Yang-Mei Chen(陈杨梅)
Chin. Phys. B, 2025, 34 (**9**): 097405. DOI: 10.1088/1674-1056/add009

SPECIAL TOPIC — John Tse: Pioneer in high-pressure materials science

Unveiling the superconducting mechanism and phase stability of LaB_2H_8 under pressure

Jirun Wu(吴际润)[1], Zefang Wang(王泽方)[1], Xin Zhong(钟鑫)[1,†], and Hanyu Liu(刘寒雨)[1,2,3,‡]

[1] *Key Laboratory of Material Simulation Methods and Software of Ministry of Education, College of Physics, Jilin University, Changchun* 130012, *China*
[2] *State Key Laboratory of High Pressure and Superhard Materials, College of Physics, Jilin University, Changchun* 130012, *China*
[3] *International Center of Future Science, Jilin University, Changchun* 130012, *China*

(Received 30 October 2025; revised manuscript received 13 January 2026; accepted manuscript online 19 January 2026)

The recent synthesis of the superhydride LaB_2H_8, which exhibits a superconducting transition temperature (T_c) of 106 K at 90 GPa, offers a promising avenue for exploring high-temperature superconductivity. However, the underlying superconducting mechanism remains elusive. Here, we employ first-principles calculations to systematically investigate the electronic structure, lattice dynamics, electron–phonon coupling, and molecular-orbital features of LaB_2H_8. Our analysis reveals that the structural stability and metallic conductivity primarily originate from the covalent B–H bonds within the B_2H_8 units. Furthermore, we observe a pronounced softening of low-frequency phonons at elevated pressures, which induces strong electron–phonon coupling and serves as the key driving force for superconductivity in this system. This work not only elucidates the superconducting mechanism in LaB_2H_8 but also highlights the importance of covalent hydrogen-based motifs in designing new high-T_c superconductors.

Keywords: first principles calculations, superconductivity, molecular orbitals

PACS: 74.25.Dw, 61.50.Ah, 62.50.–p

DOI: 10.1088/1674-1056/ae39d0 **CSTR:** 32038.14.CPB.ae39d0

1. Introduction

Superconducting materials, characterized by their zero electrical resistance and complete diamagnetism under specific conditions (typically at low temperatures), possess transformative potential across diverse fields, from medical imaging to power transmission.[1–3] The pursuit of high-temperature superconductors thus remains a central objective in condensed matter physics, motivating extensive theoretical and experimental efforts.[4–17] A major breakthrough came with the theoretical prediction by Wang *et al.*[18] of CaH_6, a hydride featuring a unique H_{24} caged framework identified via the CALYPSO structure-searching method.[19,20] This work established the hydrogen-caged framework paradigm and inaugurated a new era for hydrogen-based superconductors. The subsequent experimental synthesis of CaH_6 confirmed its exceptional superconductivity, showing a critical temperature (T_c) of 215 K at 172 GPa.[15,16] Inspired by this achievement, a growing number of theoretically predicted binary metal hydrides with clathrate structures have been experimentally verified, such as LaH_{10},[21–24] YH_6,[21,25–28] and YH_9.[21,25,26] Among them, LaH_{10} stands out, holding a record-high T_c of $\sim$ 260 K at 200 GPa.[23,24]

Driven by the goal of room-temperature superconductivity, the research field has increasingly turned to ternary hydrides. Their complex potential energy surfaces enable enhanced structural diversity, which theoretically supports more stable, high-T_c phases compared to binary hydrides. Undoubtedly, a series of clathrate ternary hydrides have emerged, revealing excellent superconducting properties.[29–36] Strikingly, a landmark achievement was reported in 2025 with the experimental synthesis of $LaSc_2H_{24}$,[33] a clathrate hydride previously predicted by Liu *et al.*[30] to host room-temperature superconductivity. The measured T_c of 298 K at 250–260 GPa confirmed this prediction, marking the first-ever realization of room-temperature superconductivity and fulfilling a long-standing dream of condensed matter physics.

Clathrate hydride-based superconductors inherently possess the gene of high-temperature and even room-temperature superconductivity. Yet the remaining challenge is their extreme synthesis pressure ($>$ 200 GPa), which hinders the path toward practical utilization. Early investigations on ternary hydrides such as $BaReH_9$[37–39] and Li_5MoH_{11}[40] uncovered a class of materials stabilized by hydrogen-based covalent units at relatively low pressures. Although these early systems exhibited only low superconducting transition temperatures ($T_c < 7$ K), they revealed a crucial insight: hydrogen-based covalent motifs can effectively stabilize hydride structures under moderate pressures, rendering them promising structural motifs for designing high-T_c superconductors under near-practical

†Corresponding author. E-mail: zhongxin@calypso.cn
‡Corresponding author. E-mail: hanyuliu@jlu.edu.cn

© 2026 Chinese Physical Society and IOP Publishing Ltd. All rights, including for text and data mining, AI training, and similar technologies, are reserved.

conditions.

Inspired by this concept, subsequent research has aimed to identify ternary hydrides that preserve such covalent frameworks while delivering higher T_c. A significant advance was achieved in 2023 with the synthesis of $LaBeH_8$,[41] which features hydrogen-based covalent molecular motifs and attains a T_c of 110 K at 80 GPa — setting a record among ternary hydrides below 100 GPa. Concurrent theoretical efforts predicted several other promising systems, such as Mg_2IrH_6,[42] predicted to have a T_c of 160 K at ambient pressure. KB_2H_8,[8] with two methane-like BH_4 units, exhibits a T_c of 134–146 K around 12 GPa by prediction. $LaBH_8$,[9,43] which is isostructural to $LaBeH_8$ and is predicted to reach a T_c of 126 K at 50 GPa, also shows enhancement attributed to the stronger covalency of the B–H bonds. These developments have naturally drawn attention to the LaBH system. In 2024, another phase in this system, LaB_2H_8 ($I4/mmm$), was experimentally synthesized.[44] This compound also incorporates B–H covalent motifs and shows a T_c of 106 K at 90 GPa. The emergence of multiple superconducting phases in the LaBH system highlights its structural versatility and reinforces the value of covalent hydrogen-based motifs in the search for high-temperature superconductors viable at near-practical pressures.

While ternary hydrides featuring covalent hydrogen motifs demonstrate impressive T_c values at moderately reduced pressures, the fundamental principles governing their stability and superconductivity continue to pose a compelling scientific question. In pursuit of answers, this work focuses on LaB_2H_8 to systematically elucidate the origins of its superconducting behavior and structural stability. Recently, our research group utilized molecular orbital (MO) analysis to explain the superconducting mechanism in the structural analog, $LaBeH_8$.[45] LaB_2H_8 likewise contains well-defined molecular units, making it an ideal candidate for a parallel MO-based investigation. Such an analysis can reveal the orbital and electron distribution within the hydrogen-rich anionic units, shedding light on the electronic foundation of its conduction behavior. A definitive understanding of this mechanism will establish a cornerstone for the rational design of new superconductors, offering valuable candidate materials to accelerate the development of practical superconducting technologies.

2. Methods

The structural optimization and electronic properties of LaB_2H_8 were calculated using the Vienna *ab Initio* simulation package (VASP),[46] which employs a plane-wave basis set within the framework of density functional theory (DFT).[47] The electron–ion interactions were described using the projector augmented wave (PAW) pseudopotential method. The Perdew–Burke–Ernzerhof (PBE)[48] exchange–correlation functional, a generalized gradient approximation (GGA) method,[49] was utilized for the electronic structure calculations. A kinetic energy cutoff of 600 eV was applied, and a Γ-centered k-point mesh with a density of $2\pi \times 0.02$ Å^{-1} was generated by the vaspkit code.[50] The k-point mesh density is $14 \times 14 \times 14$ for the primitive cell of LaB_2H_8. The bond formation analysis was performed using the integrated crystal orbital Hamiltonian population (ICOHP) method, leveraging the LOBSTER code.[51] The energy band structure was calculated along the high-symmetry path generated using the Materials Studio software. MO and their corresponding visualized wave functions in real space were derived using the vaspkit code.[50] Additionally, the electron–phonon coupling (EPC) and superconducting properties of LaB_2H_8 were investigated using density functional perturbation theory (DFPT)[52] at 210 GPa, as implemented in the Quantum-ESPRESSO (QE)[53] software package. Ultrasoft pseudopotentials[54] with a kinetic energy cutoff of 100 Ry and a charge density cutoff of 960 Ry were employed in these calculations. The charge density was integrated on a Methfessel–Paxton $28 \times 28 \times 28$ k-point mesh, and a q-point mesh of $7 \times 7 \times 7$ was used. The superconducting critical temperature (T_c) was determined using the Allen–Dynes modified McMillan equation[55] and Eliashberg equations.[56]

3. Results

3.1. Structure and electronic properties simulation

We begin by analyzing the crystal structure of the newly synthesized LaB_2H_8, which crystallizes in the $I4/mmm$ space group (Fig. 1). Within the $[B_2H_8]^{2-}$ unit, the H–H distances measure 1.64 Å and 2.05 Å, with the shortest being 1.14 Å. To further investigate the chemical bonding in LaB_2H_8, we performed simulations using the electron localization function (ELF) and the ICOHP. As shown in Fig. S1, localized electron densities are observed between H atoms separated by 1.14 Å and 1.64 Å, with corresponding ELF values of ~ 0.55 and ~ 0.57, respectively. The corresponding ICOHP values for these H–H interactions are 1.0 and 0.0 (Table S1 and Fig. 2), significantly lower than those for the B–B bond (8.2) and the B–H bonds (5.7). The ELF results (Fig. 2(b)) further confirm covalent bonding between boron and hydrogen atoms, while the lanthanum atoms engage ionically with their surrounding atoms. Collectively, the ELF and ICOHP analyses establish the $[B_2H_8]^{2-}$ unit as a covalent molecular motif, and the compound can be best described as $La^{x+}[B_2H_8]^{x-}$.

To determine the value of "x", which is crucial for understanding the electronic properties of the $[B_2H_8]^{x-}$ unit, we performed an electronic density of states (DOS) analysis. The results shown in Fig. 3(a) reveal a nearly vacant La 6s orbital, indicating the transfer of two electrons from La to the $[B_2H_8]$ unit. This leads to the conclusion that $x = 2$. At the Fermi

level (E_f), the DOS is predominantly contributed by hydrogen, a feature often associated with high-temperature superconductivity. However, structural analysis reveals that, unlike in the high-T_c superconductor LaH_{10}, the hydrogen atoms in LaB_2H_8 do not form a cage-like framework. Thus, although both systems exhibit hydrogen-dominated DOS at E_f, the underlying superconducting mechanism in LaB_2H_8 is distinct from that characteristic of hydrogen-cage superconductors such as LaH_{10} and CaH_6.

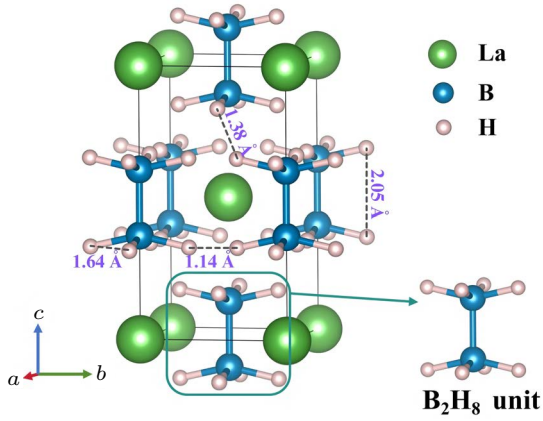


Fig. 1. The stoichiometric ternary hydride LaB_2H_8 consists of La atoms and B_2H_8 units.

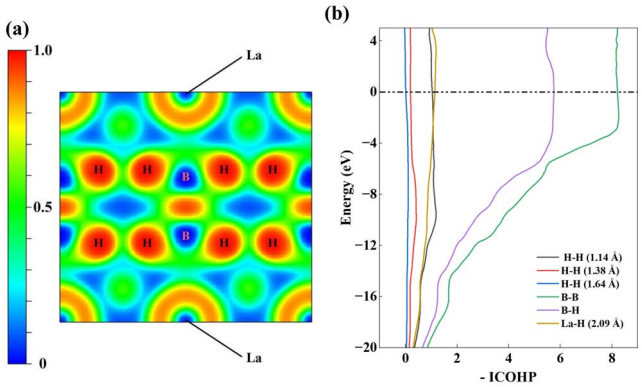


Fig. 2. (a) ELF map on the [1 0 0] crystal face. (b) ICOHP of LaB_2H_8. The dashed line indicates that B–B and B–H bonds are strong covalent bonds.

To gain a deeper understanding of the electronic properties of LaB_2H_8, we conducted electronic band structure simulations. Given the high symmetry and significant covalent character of the $[B_2H_8]^{2-}$ unit, MO theory offers an elegant framework for interpreting its electronic structure. From the calculated band structure, we extracted the real-space wave functions at the Γ point, which directly correspond to the molecular orbitals of the $[B_2H_8]^{2-}$ unit. As shown in Fig. 3(b), the molecular orbitals of the $[B_2H_8]^{2-}$ unit give rise to nine electronic bands in the energy range from -18 eV to 5 eV, with states A_{1g}, B_{2u}, A_{2u}, A_{1g}, E_g, B_{1g} and E_u. All occupied orbitals are bonding orbitals, explaining the exceptional stability of the strongly covalent $[B_2H_8]^{2-}$ unit. Notably, only two bands derived from the half-filled E_u states cross E_f, as shown in Fig. 3(c). This clarifies the metallic behavior of the compound and accounts for the dominant contribution of hydrogen to the density of states at E_f. In essence, the $[B_2H_8]^{2-}$ unit mimics the electronic behavior of atomic metallic hydrogen; therefore, the compound is endowed with the potential for superconductivity.

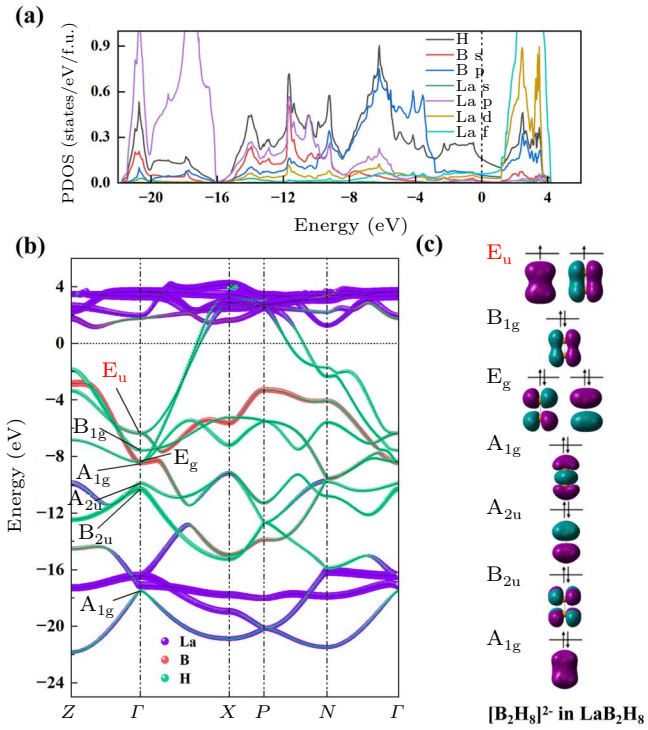


Fig. 3. (a) The orbital-projected density of states (PDOS) of LaB_2H_8 at 175 GPa. (b) Electronic band structure of LaB_2H_8. (c) MO diagram of the $[B_2H_8]^{2-}$ hydride units in LaB_2H_8. The dashed line in panels (a) and (b) indicates a hydrogen-dominated E_f. In panel (b), the radii of the colored dots are proportional to the weights of the corresponding elements. The features contributed by the $[B_2H_8]^{2-}$ units are marked at the Γ-point. In panel (c), orbitals with different angular momenta are marked with different colors.

3.2. Analysis of phonon properties and vibrational modes

To further elucidate the superconducting mechanism of LaB_2H_8, we conducted EPC simulations at 210 GPa, which yielded a T_c of 76.7 K. As illustrated in Fig. 4(a), the phonon dispersion spectrum can be divided into three distinct frequency regions (I, II, and III). Region I (0–273 cm^{-1}) comprises acoustic phonon branches dominated by vibrations of lanthanum atoms, as evidenced by the phonon density of states (PHDOS). Region II (273–1854 cm^{-1}) includes optical phonon modes predominantly arising from the vibrational motions of boron and hydrogen atoms. Analysis of the Eliashberg spectral function indicates that phonons in this region contribute approximately 70% to the total EPC, highlighting their pivotal role in mediating superconductivity. A detailed examination of the vibrational modes reveals that the dominant EPC-active phonons correspond to hydrogen vibrations perpendicular to the B–H bonds, as depicted in Fig. 4(b). Notably, phonon softening is observed primarily in region I and

the lower-frequency portion of region II (below 1200 cm^{-1}). In contrast, region III (above 2300 cm^{-1}) is characterized by high-frequency hydrogen vibrations along the B–H bond direction (Fig. 4(c)), which exhibit negligible contributions to the overall EPC. Overall, the results emphasize that the dominant EPC arises from the 273–1854 cm^{-1} range, with critical contributions from hydrogen vibrations perpendicular to the B–H bonds. This low-frequency phonon softening, coupled with the directional nature of hydrogen motion, is instrumental in facilitating superconductivity in LaB_2H_8.

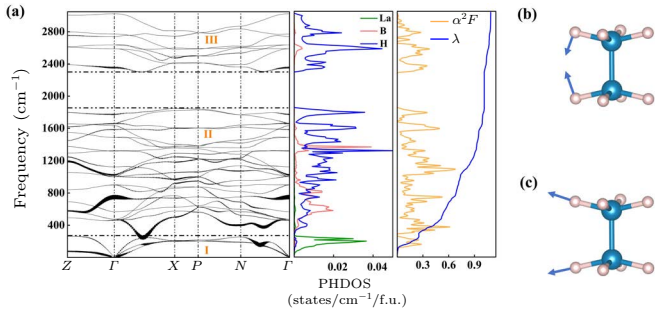


Fig. 4. (a) Phonon dispersion, element-projected phonon density of states (PHDOS), and Eliashberg spectral function of LaB_2H_8 at 210 GPa. (b) and (c) are vibrational modes perpendicular to and along the B–H bond direction, respectively.

To make a clear comparison, we have also examined KB_2H_8, which has a T_c of 134–146 K at 12 GPa.[8] Although its stoichiometric formula is similar to that of LaB_2H_8, their electrical conduction mechanisms are entirely different. In KB_2H_8, boron and hydrogen form BH_4 units with a methane-like structure, rather than the extended B_2H_8 unit found in LaB_2H_8. We performed a DOS calculation for KB_2H_8 (Fig. S3) and found that the K 4s orbitals are almost zero at the Fermi level, indicating that each K atom donates one electron to two BH_4 units. According to the Valence shell electron pair repulsion (VSEPR) theory,[57,58] each BH_4 unit requires, on average, one electron to achieve a methane-like configuration. However, in KB_2H_8, only two BH_4 units share one electron on average, suggesting that the BH_4 units are still electron-deficient. We then replaced K with Ca and calculated the DOS of CaB_2H_8 (Fig. S4). The results reveal that CaB_2H_8 is a semiconductor. Thus, the electrical conductivity of KB_2H_8 and the dominance of B and H states near the Fermi level originate from hole doping.

We further analyzed the EPC in KB_2H_8 (Fig. 5). Its phonon frequencies are generally lower than those in LaB_2H_8 and can also be divided into three regions: acoustic branches (region I), optical branches involving H vibrations relative to B–H bonds (region II, 161–1000 cm^{-1}), and optical branches with B–H bond-stretching modes (region III). In KB_2H_8, the frequencies in region II range from 161 cm^{-1} to 1000 cm^{-1}, which are much lower than those in region II of LaB_2H_8. Regarding the contribution to EPC, the low-frequency region of KB_2H_8 plays a more significant role, with more pronounced phonon softening in the acoustic branch, particularly near the Γ and X points. The phonon softening near the Γ point involves vibrations of K, B, and H atoms, while the softening near the X point is mainly due to K and H vibrations. These two regions show much greater phonon softening than other points, which is not observed in LaB_2H_8. Region I contributes over 33% to overall EPC, while the contribution from region III is negligible. Thus, the superconducting mechanisms of these two compounds are different.

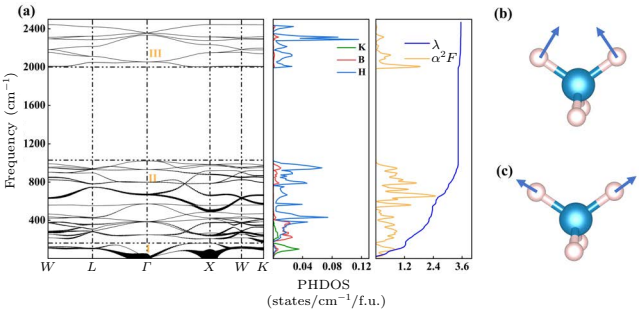


Fig. 5. (a) Phonon dispersion, element-projected phonon density of states (PHDOS), and Eliashberg spectral function of KB_2H_8 at 12 GPa. (b) and (c) are vibrational modes perpendicular to and along the B–H bond direction, respectively.

4. Conclusion and perspectives

To conclude, our comprehensive investigation demonstrates that LaB_2H_8 can be conceptualized as a salt-like compound, formulated as $La^{2+}[B_2H_8]^{2-}$, wherein the covalent $[B_2H_8]^{2-}$ unit dictates both the structural and superconducting properties. The emergence of conductivity and a hydrogen-rich Fermi level arises from the partial occupancy of hydrogen-derived E_u states within the $[B_2H_8]^{2-}$ unit. The pronounced stability is rationalized by the fact that all occupied molecular orbitals are bonding orbitals. Furthermore, EPC calculations indicate that vibrational modes perpendicular to the B–H bonds play a critical role in mediating the EPC interactions responsible for superconductivity. These insights provide a fundamental understanding of the stability and high-T_c mechanism in LaB_2H_8, while also providing a theoretical blueprint for low-pressure ternary and even multinary hydride superconductors incorporating covalent hydrogen frameworks.

Acknowledgments

Project supported by the National Key Research and Development Program of China (Grant Nos. 2023YFA1406002 and 2023YFA1608901), the National Natural Science Foundation of China (Grant Nos. 12574012, 12374009, and T2495231), the Program for Jilin University Science and Technology Innovative Research Team (Grant No. 2021TD-05), the Program for Jilin University Computational Interdisciplinary Innovative Platform, the Strategic Priority Research Program of the Chinese Academy of Sciences (Grant

No. XDB33000000), the Fundamental Research Funds for the Central Universities, and computing facilities at the High-Performance Computing Centre of Jilin University, and the Graduate Innovation Fund of Jilin University (Grant No. 2025CX090).

References

[1] Orenstein J and Millis A J 2000 *Science* **288** 468
[2] Scanlan R M, Malozemoff A P and Larbalestier D C 2004 *Proc. IEEE* **92** 1639
[3] Simon A 1997 *Angew. Chem. Int. Ed. Engl.* **36** 1788
[4] Zhang Z, Cui T, Hutcheon M J, Shipley A M, Song H, Du M, Kresin V Z, Duan D, Pickard C J and Yao Y 2022 *Phys. Rev. Lett.* **128** 047001
[5] Li S, Wang H, Sun W, Lu C and Peng F 2022 *Phys. Rev. B* **105** 224107
[6] Liang X, Bergara A, Wang L, Wen B, Zhao Z, Zhou X, He J, Gao G and Tian Y 2019 *Phys. Rev. B* **99** 100505
[7] Jiang Q, Zhang Z, Song H, Ma Y, Sun Y, Miao M, Cui T and Duan D 2024 *Fundam. Res.* **4** 550
[8] Gao M, Yan X W, Lu Z Y and Xiang T 2021 *Phys. Rev. B* **104** L100504
[9] Di Cataldo S, Heil C, Von Der Linden W and Boeri L 2021 *Phys. Rev. B* **104** L020511
[10] Di Cataldo S, Von Der Linden W and Boeri L 2022 *npj Comput. Mater.* **8** 2
[11] Lucrezi R, Di Cataldo S, Von Der Linden W, Boeri L and Heil C 2022 *npj Comput. Mater.* **8** 119
[12] Ma T, Zhang Z, Du M, Huo Z, Chen W, Tian F, Duan D and Cui T 2023 *Mater. Today Phys.* **38** 101233
[13] Sun Y, Wang Y, Zhong X, Xie Y and Liu H 2022 *Phys. Rev. B* **106** 024519
[14] Liu L, Peng F, Song P, Liu X, Zhang L, Huang X, Niu C, Liu C, Zhang W, Jia Y and Zhang Z 2023 *Phys. Rev. B* **107** L020504
[15] Ma L, Wang K, Xie Y, Yang X, Wang Y, Zhou M, Liu H, Yu X, Zhao Y, Wang H, Liu G and Ma Y 2022 *Phys. Rev. Lett.* **128** 167001
[16] Li Z, He X, Zhang C, Wang X, Zhang S, Jia Y, Feng S, Lu K, Zhao J, Zhang J, Min B, Long Y, Yu R, Wang L, Ye M, Zhang Z, Prakapenka V, Chariton S, Ginsberg P A, Bass J, Yuan S, Liu H and Jin C 2022 *Nat. Commun.* **13** 2863
[17] Sun Y, Wu J, Yang L, Zhang S, Zhong X and Liu H 2025 *Comput. Mater. Today* **7** 100035
[18] Wang H, Tse J S, Tanaka K, Iitaka T and Ma Y 2012 *Proc. Natl. Acad. Sci. USA* **109** 6463
[19] Wang Y, Lv J, Zhu L and Ma Y 2012 *Comput. Phys. Commun.* **183** 2063
[20] Wang Y, Lv J, Zhu L and Ma Y 2010 *Phys. Rev. B* **82** 094116
[21] Peng F, Sun Y, Pickard C J, Needs R J, Wu Q and Ma Y 2017 *Phys. Rev. Lett.* **119** 107001
[22] Liu H, Naumov I I, Hoffmann R, Ashcroft N W and Hemley R J 2017 *Proc. Natl. Acad. Sci. USA* **114** 6990
[23] Laniel D, Trybel F, Winkler B, Knoop F, Fedotenko T, Khandarkhaeva S, Aslandukova A, Meier T, Chariton S, Glazyrin K, Milman V, Prakapenka V, Abrikosov I A, Dubrovinsky L and Dubrovinskaia N 2022 *Nat. Commun.* **13** 6987
[24] Somayazulu M, Ahart M, Mishra A K, Geballe Z M, Baldini M, Meng Y, Struzhkin V V and Hemley R J 2019 *Phys. Rev. Lett.* **122** 027001
[25] Kong P, Minkov V S, Kuzovnikov M A, Drozdov A P, Besedin S P, Mozaffari S, Balicas L, Balakirev F F, Prakapenka V B, Chariton S, Knyazev D A, Greenberg E and Eremets M I 2021 *Nat. Commun.* **12** 5075
[26] Wang Y, Wang K, Sun Y, Ma L, Wang Y, Zou B, Liu G, Zhou M and Wang H 2022 *Chin. Phys. B* **31** 106201
[27] Li Y, Hao J, Liu H, Tse J S, Wang Y and Ma Y 2015 *Sci Rep* **5** 9948
[28] Troyan I A, Semenok D V, Kvashnin A G, *et al.* 2021 *Adv. Mater.* **33** 2006832
[29] He X L, Zhang P, Ma Y, Li H, Zhong X, Wang Y, Liu H and Ma Y 2023 *Phys. Rev. B* **107** 134509
[30] He X L, Zhao W, Xie Y, Hermann A, Hemley R J, Liu H and Ma Y 2024 *Proc. Natl. Acad. Sci. USA* **121** e2401840121
[31] An D, Conway Lewis J, Duan D, Zhang Z, Jiang Q, Song H, Huo Z, Pickard C J and Cui T 2025 *Adv. Funct. Mater.* **35** 2418692
[32] Zhao W, Duan D, Du M, Yao X, Huo Z, Jiang Q and Cui T 2022 *Phys. Rev. B* **106** 014521
[33] Song Y, Ma C, Wang H, Zhou M, Qi Y, Cao W, Li S, Liu H, Liu G and Ma Y 2025 *arXiv* arXiv:2510.01273
[34] Sun Y, Lv J, Xie Y, Liu H and Ma Y 2019 *Phys. Rev. Lett.* **123** 097001
[35] Du M, Song H, Zhang Z, Duan D and Cui T 2022 *Research* **2022** 20229784309
[36] Sun Y, Wang Y, Zhong X, Xie Y and Liu H 2022 *Phys. Rev. B* **106** 024519
[37] Markopoulos G, Kroll P and Hoffmann R 2010 *J. Am. Chem. Soc.* **132** 748
[38] Muramatsu T, Wanene W K, Somayazulu M, Vinitsky E, Chandra D, Strobel T A, Struzhkin V V and Hemley R J 2015 *J. Phys. Chem. C* **119** 18007
[39] Vinitsky E A, Muramatsu T, Somayazulu M, Wanene W K, Liu Z, Chandra D and Hemley R J 2016 *J. Phys.: Condens. Matter* **28** 505701
[40] Meng D, Sakata M, Shimizu K, Iijima Y, Saitoh H, Sato T, Takagi S and Orimo S 2019 *Phys. Rev. B* **99** 024508
[41] Song Y, Bi J, Nakamoto Y, Shimizu K, Liu H, Zou B, Liu G, Wang H and Ma Y 2023 *Phys. Rev. Lett.* **130** 266001
[42] Dolui K, Conway L J, Heil C, Strobel T A, Prasankumar R P and Pickard C J 2024 *Phys. Rev. Lett.* **132** 166001
[43] Liang X, Bergara A, Wei X, Song X, Wang L, Sun R, Liu H, Hemley R J, Wang L, Gao G and Tian Y 2021 *Phys. Rev. B* **104** 134501
[44] Song X, Hao X, Wei X, He X L, Liu H, Ma L, Liu G, Wang H, Niu J, Wang S, Qi Y, Liu Z, Hu W, Xu B, Wang L, Gao G and Tian Y 2024 *J. Am. Chem. Soc.* **146** 13797
[45] Wang Z, Zhao H J, Zhong X, Liu H and Ma Y 2024 *Phys. Rev. B* **109** 214506
[46] Kresse G and Furthmüller J 1996 *Phys. Rev. B* **54** 11169
[47] Blöchl P E 1994 *Phys. Rev. B* **50** 17953
[48] Perdew J P and Wang Y 1992 *Phys. Rev. B* **45** 13244
[49] Perdew J P, Burke K and Ernzerhof M 1996 *Phys. Rev. Lett.* **77** 3865
[50] Wang V, Xu N, Liu J C, Tang G and Geng W T 2021 *Comput. Phys. Commun.* **267** 108033
[51] Deringer V L, Tchougréeff A L and Dronskowski R 2011 *J. Phys. Chem. A* **115** 5461
[52] Baroni S, De Gironcoli S, Dal Corso A and Giannozzi P 2001 *Rev. Mod. Phys.* **73** 515
[53] Giannozzi P, Baroni S, Bonini N, *et al.* 2009 *J. Phys.: Condens. Matter* **21** 395502
[54] Kresse G and Joubert D 1999 *Phys. Rev. B* **59** 1758
[55] Allen P B and Dynes R C 1975 *Phys. Rev. B* **12** 905
[56] Eliashberg G M 1960 *Sov. Phys. JETP* **11** 696
[57] Gillespie R J and Nyholm R S 1957 *Q. Rev. Chem. Soc.* **11** 339
[58] Gillespie R J 1963 *J. Chem. Educ.* **40** 295